ISBN: 978-3-95450-179-3 doi:10.18429/JACoW-FEL2017-MOP020

SIDEBAND INSTABILITY IN A TAPERED FREE ELECTRON LASER*

Cheng-Ying Tsai[1†], Juhao Wu[1‡], Chuan Yang[1,2], Moohyun Yoon[1,3], and Guanqun Zhou[1,4]
[1]SLAC National Accelerator Laboratory, Menlo Park, USA
[2]NSRL, University of Science and Technology of China, Hefei, Anhui, China
[3]Department of Physics, Pohang University of Science and Technology, Pohang, Korea
[4]Institute of High Energy Physics, and UCAS, Chinese Academy of Sciences, Beijing, China

Abstract

For a high-gain tapered free electron laser (FEL), it is known that there is a so-called second saturation point where the FEL power growth stops. Sideband instability is one of the major reasons leading to this second-saturation and thus prevents from reaching hundreds of gigawatt (GW) or even terawatt (TW) level power output in an x-ray FEL. It was believed that a strong taper can effectively suppress the sideband instability and further improves the efficiency and peak power. In this paper, we give quantitative analysis of the dependence of taper gradient on the sideband growth. The study is carried out semi-analytically together with numerical simulation. The numerical parameters are taken from LCLS-like electron bunch and undulator system. The results confirm the effectiveness of strong undulator tapering on sideband suppression.

INTRODUCTION

Free electron laser (FEL) is known to be capable of generating coherent high-power radiation over a broad range of spectrum. In the x-ray FEL regime, the power efficiency is about 10^{-3}, indicating that the first saturated power can be ~50 GW for electron beam with peak current ~5 kA and energy ~10 GeV operating in the self-amplified spontaneous emission (SASE) mode in a ~100-m-long untapered undulator. With undulator tapering, the efficiency can be improved and the power can be further increased in the post-saturation regime but eventually will reach a so-called second saturation and the radiation then approaches another equilibrium. Although numerical simulations show that the TW level of temporally integrated FEL power can be possible when the undulator tapering (of helical type) is optimized and the self-seeded scheme is employed [1], in the post-saturation regime it is the sideband instability that still limits the growth of the main signal [2–6]. Enhancing the FEL peak power can be envisioned once the sideband instability is effectively suppressed. Such instability in FELs is caused by the interaction of the electromagnetic field with the electron synchrotron motion in the ponderomotive potential well. The potential well, formed by the undulator field and the main signal, will trap electrons and result in oscillation with a synchrotron frequency (and its multiples) away from the resonance or main-signal frequency. Once the interaction creates a positive feedback, the electron beam energy will transfer and contribute to the electromagnetic field with the synchrotron sideband frequency. Then the sideband signal will grow and usually bring about undesirable consequences. In this paper we will focus on the sideband instability in a single-pass high-gain tapered FEL in the post-saturation regime based on single-particle description in a one-dimensional (1-D) model. The validity of 1-D analysis assumes that the transverse size of the electron beam is large compared with that of the radiation field, thus ignoring the effects of diffraction and gradient of transverse electron beam density. Using a single-particle approach, we can obtain the corresponding dispersion equation, which accounts for sideband-related dynamical quantities. Then, by quantifying the so-called sideband field gain, we compare the theoretical predictions with the results from a 1-D FEL simulation and they show good agreement. We particularly focus on the effect of undulator tapering on the sideband growth and study both the gentle and strong undulator tapering, compared with the untapered case. Our numerical simulations are based on similar parameters to those of the Linac Coherent Light Source (LCLS), the LCLS-like parameters.

THEORETICAL FORMULATION

In 1-D FEL, the main signal is governed by the resonance condition, $\lambda_R = \frac{\lambda_u}{2\gamma_R^2(z)}\left(1+\frac{K^2(z)}{2}\right)$, where λ_u is the undulator period, λ_R is the radiation wavelength of the main signal, γ_R is the electron reference energy in unit of its rest mass energy, $K \approx 0.934 B_0[\text{Tesla}]\lambda_u[\text{cm}]$ is the (peak) undulator parameter, and B_0 the peak undulator magnetic field. Here λ_u is assumed constant, and K is in general a function of the undulator axis z with $B(z) = B_0 f_B(z)$ and $f_B(z)$ is the tapering profile. The 1-D FEL process can be formulated based on the following electron dynamics and wave equations [7, 8]:

$$\frac{d\theta}{d\hat{z}} = \frac{\partial \mathcal{H}}{\partial \eta} = \frac{\eta - \eta_R}{f_R}, \tag{1}$$

$$\frac{d\eta}{d\hat{z}} = -\frac{\partial \mathcal{H}}{\partial \theta} = -\frac{f_B}{f_R}\left(\mathcal{E}e^{i\theta} + \mathcal{E}^* e^{-i\theta}\right), \tag{2}$$

and

$$\frac{d\mathcal{E}}{d\hat{z}} = \left(\frac{\partial}{\partial \hat{z}} + \frac{\partial}{\partial \hat{u}}\right)\mathcal{E} = \frac{f_B}{f_R}\left\langle e^{-i\theta}\right\rangle. \tag{3}$$

In the equations, $\theta = (k_R + k_u)z - \omega_R t$ is the electron phase with respect to the radiation, and $\eta \equiv (\gamma - \gamma_R(0))/\rho\gamma_R(0)$

* The work was supported by the US Department of Energy (DOE) under contract DE-AC02-76SF00515 and the US DOE Office of Science Early Career Research Program grant FWP-2013-SLAC-100164.
† jcytsai@SLAC.Stanford.EDU
‡ jhwu@SLAC.Stanford.EDU

ISBN: 978-3-95450-179-3 doi:10.18429/JACoW-FEL2017-MOP020

is the normalized energy deviation with respect to the dimensionless FEL or Pierce parameter ρ. In the case of undulator tapering, the electron reference energy is modified accordingly through the resonance condition to be $\gamma_R(z) = \gamma_{R0} f_R(z)$ where $f_R(z) = \sqrt{(1 + K^2(z)/2)/(1 + K_0^2/2)}$. $|\mathcal{E}| = |E| \Big/ \sqrt{4\pi n_0 \rho \gamma_{R0} m_0 c^2}$ is the normalized amplitude of the electric field E. Other relevant quantities are normalized as $\hat{z} = 2k_u \rho z$, $\hat{s} = 2k_u \rho (z - \beta_z ct)$ with $k_u = 2\pi/\lambda_u$, $k_R = 2\pi/\lambda_R$, $\omega_R = ck_R$, $\beta_z = v_z/c$, and $\hat{u} = \hat{s}/(1 - \beta_z)$. Equation (3) is obtained by taking the slowly varying envelope approximation and the bracket $\langle ... \rangle$ denotes the ensemble average over the electron beam phases. Inserting $\mathcal{E} = |\mathcal{E}_0| e^{i\phi}$ into Eq. (3) and letting $\Theta = \theta + \phi$ will give two separate equations for the amplitude and phase of the radiation field to the zeroth order:

$$\frac{\partial}{\partial \hat{z}} + \frac{\partial}{\partial \hat{u}} \; |\mathcal{E}_0| = \frac{f_B}{f_R} \cos\Theta, \tag{4}$$

and

$$|\mathcal{E}_0| \frac{\partial \phi}{\partial \hat{z}} = -\frac{f_B}{f_R} \sin\Theta. \tag{5}$$

For the case of the untapered FEL, the field amplitude after saturation is constant (or oscillates around an equilibrium) and the radiation phase ϕ is linear in z. In what follows, the main signal is determined by the conservation of energy, where the field amplitude is given by $|\mathcal{E}_0| = \sqrt{\left|\mathcal{E}_0^{(0)}\right|^2 + (1 - f_R(\hat{z}))/\rho}$, where $\mathcal{E}_0^{(0)}$ is evaluated at the location of the first saturation and we have presumed $\cos\Theta \approx \cos\Theta_R$. Now we can study the stability of such a 1-D FEL system. Since we are interested in the sideband instability after the first saturation, we will Taylor expand the dynamical quantities around their saturation equilibria and study how the perturbation affects the system. Let us assume

$$\begin{aligned} \mathcal{E} &= (|\mathcal{E}_0| + \delta\mathcal{E}' + i\delta\mathcal{E}'') e^{i\phi}, \\ \eta &= \eta_R + \delta\eta, \\ \text{and } \theta &= \theta_R + \delta\theta, \end{aligned} \tag{6}$$

where $\theta_R = \Theta_R - \phi$. The quantities with δ ahead are considered to be small and sideband-related quantities. Linearizing Eqs. (1) and (2) using the third relation of Eq. (6) lead to the small-amplitude electron synchrotron motion with $\Omega_{\rm syn}^2 = -2\frac{f_B}{f_R^2} |\mathcal{E}| \sin\Theta_R$. Next, we presume these perturbations do not interact with each other and behave as $(\delta\theta, \delta\eta, \delta\mathcal{E}', \delta\mathcal{E}'') \propto e^{ik\hat{z} - i\kappa\hat{u}}$, where κ is assumed real and k can be in general complex. The real part of k represents the propagation constant, while the imaginary part indicates the growth (or damping) of the associated quantities. Inserting into Eqs.(1), (2), and (4) will result in a set of linear equations. The stability is then determined by the determinant of the corresponding coefficient matrix, i.e. the dispersion relation:

$$\left(k^2 - \Omega_{\rm syn}^2\right) \left[(k - \kappa)^2 - \frac{f_R^2}{4|\mathcal{E}_0|^4} \Omega_{\rm syn}^4\right] - \frac{f_B^2}{f_R^2 |\mathcal{E}_0|^2} \Omega_{\rm syn}^2 = 0. \tag{7}$$

In this equation we will solve for k provided κ is given. The general behavior of the imaginary part of k, $\mathrm{Im}k < 0$, features the growth of the sideband signal, where the maximum growth rate occurs at $\kappa \approx \Omega_{\rm syn}(\hat{z})$, shown in Fig. 1. There exists a cutoff threshold for κ, above which the oscillating electron beam will not interact the corresponding spectral components and the corresponding signals do not exist.

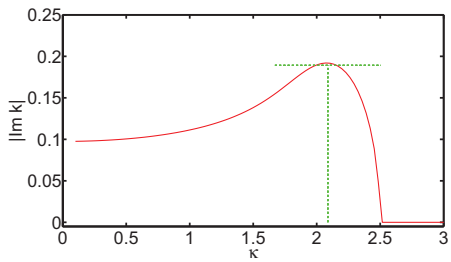

Figure 1: The growth rate $|\mathrm{Im}k|$ as a function of κ. The dispersion curve is solved for the case of $\Omega_{\rm syn} \approx 2$, $|\mathcal{E}_0| \approx 10$, and $f_B = f_R = 1$. The maximum growth rate $\max|\mathrm{Im}k|$ occurs at $\kappa \approx \Omega_{\rm syn}$.

An approximate analytical expression for the maximum growth rate can be found by looking for $k = \Omega_{\rm syn} + \delta k$, where δk is in general a complex quantity and letting $d^2\delta k \,/\, d\kappa^2 = 0$, giving [3, 8]:

$$\max|\mathrm{Im}k| \approx \frac{\sqrt{3}}{2} \left[\frac{f_B^2(\hat{z}) \Omega_{\rm syn}(\hat{z})}{2 f_R^2(\hat{z}) |\mathcal{E}_0(\hat{z})|^2}\right]^{1/3}. \tag{8}$$

NUMERICAL RESULTS

In this section we will compare the numerical solutions of Eq. (7) with the full 1-D FEL simulation results [9]. Table 1 summarizes the relevant parameters for a LCLS-like hard x-ray self-seeding (HXRSS) configuration. To compare the theoretical prediction with the 1-D FEL simulation, we need to analyze the FEL output spectra. The readers are referred to Ref. [10] for the details. We define the sideband field gain as $G(\hat{z}) \equiv \left|\frac{\mathcal{E}_s(\hat{z})}{\mathcal{E}_s(\hat{z}_0)}\right| = e^{\Lambda\hat{z}}$, where $\mathcal{E}_s$ is the sideband field around $\omega_s \approx 2\gamma_R^2 c\Omega_{\rm syn}$, $\hat{z}_0$ is at the first saturation, and Λ is the (z-integrated) sideband field growth rate. In what follows we are mostly interested in the third (last) section of LCLS undulator, which consists of a total of 16 undulator segments (the 17th to 32nd undulators) with the total length about 50 m. The initial saturation occurs at $z \approx 13$ m (not shown here) for all three different cases: no taper, gentle (0.8%) and strong (10%) undulator taperings. Now let us look at the effect of different undulator taperings on the sideband instability gain. Figure 2 illustrates the three different situations. From (a-c) we see that both the

ISBN: 978-3-95450-179-3 doi:10.18429/JACoW-FEL2017-MOP020

Table 1: Numerical Parameters for the Beam, Undulator and Radiation Fields for the Hard X-Ray FELs

Name	Value	Unit
Electron beam energy	10.064	GeV
RMS relative energy spread	10^{-4}	
Peak current	4	kA
Normalized emittances (x, y)	0.3,0.3	μm-rad
Average beta function (x, y)	5,5	m
Undulator parameter K_0 (peak)	3.5	
Undulator period	3	cm
Input seed power	1	MW
Resonance wavelength	2.755/4.5	Å/keV
First saturation power	~80	GW
First saturation length	~13	m

theoretical predictions and the 1-D FEL simulation results match reasonably well. In particular, we find that as the taper ratio increases, the sideband field gains become reduced. Comparing Fig. 2(a,b) with (c), there is also an interesting observation that the lower sideband dominates in the untapered or gentle-tapered case while the upper sideband may, but not necessarily, dominate in the strong undulator tapering. Here the theoretical prediction can not distinguish whether the lower or upper sideband will dominate because of employment of the single-particle description [1]. From Fig. 2 it appears that the theoretical predictions overall match the dominant sideband very well. Moreover, the otherwise dominant sideband has always smaller growth rate and will be of less concern. Having compared the sideband field gains, let us examine the evolution of FEL output spectra for the three different undulator taperings. From Fig. 2(d-f), it can be found that the main signal with 0.8% taper ratio increases about 2.5 times of that with the untapered case. Moreover, the sideband field for the case of 0.8% undulator tapering is comparable to that of untapered case. The increase of the main signal due to undulator tapering also results in the increase of synchrotron sideband frequency. Thus the sampling synchrotron sideband frequency (marked as thin green lines) over the tapered FEL output spectrum spans a wider range than that of the untapered case. It can be even wider for larger taper ratio. The thick green lines in the figure are used to indicate the final synchrotron sideband frequency at the undulator exit (only lower sideband is shown). For the untapered case, the sampling synchrotron sideband frequency does in fact move back and forth within a certain sideband spectral range because of the periodic oscillation of the saturation power about an equilibrium. The back-and-forth sampling will result in accumulation of sideband field gain. When increasing the ratio of undulator tapering, the sideband spectrum will become broadened and the corresponding sideband field gain will reduce.

[1] Such an asymmetric sideband spectrum, either lower or upper sideband will dominate, can indeed depend on the detailed electron distribution in the phase space. More specifically, it can be possible that not the entire range of the upper or lower sideband spectrum will dominate against the other.

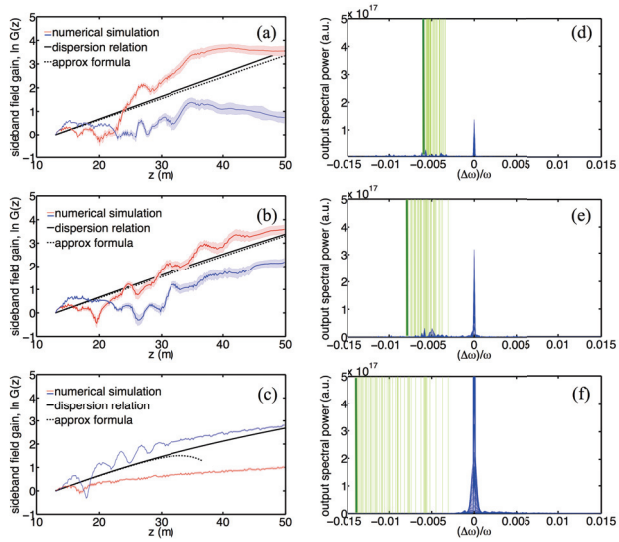

Figure 2: Sideband field gain $\ln G(z)$ as a function of z (left column) and FEL output spectra at undulator exit (right column), for (a,d) untapered, (b,e) 0.8%-tapered, and (c,f) 10%-tapered cases. For (a-c) the numerical simulations are averaged results out from 50 independent runs. For (d-f) only the lower-sideband portion is plotted; while the upper-sideband will be symmetrical should we plot it.

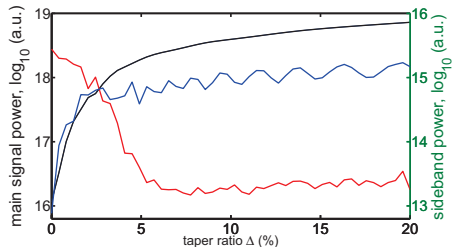

Figure 3: The main signal and the sideband power (in logarithmic scale) as a function of the taper ratio. In the axis of sideband power, the red and blue refer to the lower and upper sideband powers, respectively. The curves in this figure are obtained from the averaged results of 50 independent runs for each taper ratio.

SUMMARY AND CONCLUSION

In this work, we have derived the 1-D FEL sideband dispersion relation [7, 8] and obtained approximate analytical formulas for the maximum sideband growth rate (see Ref. [10] for more details). The instantaneous growth rate can serve as a quick estimate for the FEL sideband effect. Then we studied the FEL sideband effects based on LCLS-like parameters and have investigated the dependence of the sideband instability growth rate on the undulator taper ratio. We find that the undulator tapering can have mitigating effect on sideband growth, through the direct taper ratio, while the increase of the main signal due to the undulator tapering will make the reduction become ineffective. Using numerical simulations it can be found that 10% appears to be passable for both maximizing the main signal and reducing the lower sideband signal. In the meantime the upper sideband begins to emerge around $\Delta \approx 2\%$, at a however slightly smaller ratio than the lower sideband field being appreciably dropped.

ISBN: 978-3-95450-179-3 doi:10.18429/JACoW-FEL2017-MOP020

Figure 3 shows the dependence of the main signal power and the sideband field gains as a function of the taper ratio. Not shown here but the similar conclusion is also drawn when we use 3-D numerical simulation [11].

REFERENCES

[1] J. Wu, N. Hu, H. Setiawan, X. Huang, T. O. Raubenheimer, Y. Jiao, G. Yu, A. Mandlekar, S. Spampinati, K. Fang, C. Chu, and J. Qiang, "Multi-dimensional optimization of a terawatt seeded tapered free electron laser with a multi-objective genetic algorithm", *Nuclear Instruments and Methods in Physics Research Section A: Accelerators, Spectrometers, Detectors and Associated Equipment*, 846:56, 2017.

[2] N. Kroll, P. Morton, and M. Rosenbluth, "Free-electron lasers with variable parameter wigglers.", *IEEE Journal of Quantum Electronics,* 17(8):1436-1468, August 1981.

[3] Ronald C. Davidson and Jonathan S. Wurtele, "Single-particle analysis of the free-electron laser sideband instability for primary electromagnetic wave with constant phase and slowly varying phase", *The Physics of Fluids*, 30(2):557-569, 1987.

[4] W. M. Sharp and S. S. Yu, "Two-dimensional Vlasov treatment of free-electron laser sidebands", *Physics of Fluids B: Plasma Physics*, 2(3):581-605, 1990.

[5] Ravi P. Pilla and A. Bhattacharjee, "Elimination of the sideband instability in variable parameter free electron lasers and inverse free electron lasers", *Physics of Plasmas*, 1(2):390-397, 1994.

[6] Spilios Riyopoulos, "Sideband suppression in tapered wiggler free electron lasers including thermal spreads", *Physics of Plasmas*, 7(5):1586-1594, 2000.

[7] R. Bonifacio, F. Casagrande, M. Ferrario, P. Pierini, and N. Piovella, "Hamiltonian model and scaling laws for free-electron-laser amplifiers with tapered wiggler", *Optics Communications*, 66(2):133-139, 1988.

[8] S. Isermann and R. Graham, "Suppression of the sideband instability in tapered free-electron lasers", Physical Review A, 45:4050, 1992.

[9] K.-J. Kim, Z. Huang and R. Lindberg, "Synchrotron Radiation and Free-Electron Lasers: Principles of Coherent X-Ray Generation", Cambridge University Press, 2017.

[10] C.-Y. Tsai, J.Wu, C. Yang, M. Yoon, and G. Zhou, Analysis of the sideband instability based on an one-dimensional high-gain free electron laser model, submitted to *Phys. Rev. Accel. Beams*, 2017.

[11] S. Reiche, "GENESIS 1.3: a fully 3D time-dependent FEL simulation code", *Nuclear Instruments and Methods in Physics Research Section A: Accelerators, Spectrometers, Detectors and Associated Equipment*, vol. 429, pp. 243-248, 1999.